

Article

Exploring the Physicochemical and Antioxidant Characteristics of Honey from Eastern Morocco: Insights into Potential Health Benefits and Molecular Docking Analysis

Azzedine Abeslami ¹, Hammadi El Farissi ^{1,*}, Ali El Bachiri ¹, Mariane Sindic ², Marie-Laure Fauconnier ³, Etienne Bruneau ⁴ and Abdelmonaem Talhaoui ¹

- ¹ Laboratory of Environment and Applied Chemistry (LCAE), Team: Physical Chemistry of the Natural Resources and Processes, Faculty of Sciences, Mohammed First University, Oujda 60000, Morocco
- ² Laboratory of Agro-Food Quality and Safety, Faculty of the Agronomic Sciences, University Liege of Gembloux Agro-Bio Tech, Beekeeping Research and Information Centre (CARI), 1348 Louvain-la-Neuve, Belgium
- ³ Laboratory of Chemistry of Natural Molecules, Gembloux Agro-Bio Tech, Liege University, Passage des Déportés 2, 5030 Gembloux, Belgium; marie-laure.fauconnier@uliege.be
- ⁴ Beekeeping Research and Information Centre (CARI), 1348 Louvain-la-Neuve, Belgium
- * Correspondence: hammadi.elfarissi@ump.ac.ma; Tel.: +212-690-963-463

Abstract: This study evaluates the physicochemical properties, phenolic and flavonoid content, antioxidant activity, and molecular docking interactions of honey from eastern Morocco. Analysis confirmed compliance with European Commission standards, with moisture content ranging from 15.39% to 19.74% and pH between 3.79 and 4.94. Carob honey exhibited the highest protein content (0.42%), polyphenol concentration (720.16 mg gallic acid/kg), flavonoid content (90.5 mg catechin/kg), and antioxidant activity (63.5% DPPH inhibition). Strong correlations were observed between phenolic and flavonoid content and antioxidant properties. Molecular docking identified ethyl phenylacetate and thymol as key compounds with significant interactions with cytochrome c peroxidase, suggesting potential therapeutic effects. DFT calculations supported these findings, indicating these compounds may enhance antioxidant activity. The study highlights the exceptional quality and antioxidant capacity of honey from eastern Morocco, reflecting its unique floral sources and potential as a natural source of antioxidants with therapeutic benefits.

Keywords: eastern Morocco honey; antioxidant activity; physicochemical properties; total phenolic content; total flavonoid content; molecular docking; DFT



Citation: Abeslami, A.; El Farissi, H.; El Bachiri, A.; Sindic, M.; Fauconnier, M.-L.; Bruneau, E.; Talhaoui, A. Exploring the Physicochemical and Antioxidant Characteristics of Honey from Eastern Morocco: Insights into Potential Health Benefits and Molecular Docking Analysis. *Agriculture* **2024**, *14*, 1540. <https://doi.org/10.3390/agriculture14091540>

Agriculture **2024**, *14*, 1540. <https://doi.org/10.3390/agriculture14091540>

Academic Editor: Vita Di Stefano

Received: 30 July 2024

Revised: 28 August 2024

Accepted: 4 September 2024

Published: 6 September 2024



Copyright: © 2024 by the authors. Licensee MDPI, Basel, Switzerland. This article is an open access article distributed under the terms and conditions of the Creative Commons Attribution (CC BY) license (<https://creativecommons.org/licenses/by/4.0/>).

1. Introduction

The properties of honey differ from region to region, leading to investigations into the distinctive characteristics of honey from eastern Morocco compared to other areas. This knowledge is vital for consumers and industries interested in its potential for pharmaceuticals and functional foods [1,2]. Honey's attributes, influenced by ecological factors and plant origins, exhibit diverse phenol levels impacting antioxidant activity [3–7]. Additionally, processing and storage conditions impact its composition. Honey is well-known for its medicinal benefits, and is recommended for various groups, aiding bodily functions and combating free radicals due to its high antioxidant content. Research indicates that consuming honey can enhance plasma antioxidant activity, potentially offering protection against oxidative stress, which fuels ongoing studies into its antioxidant properties across different botanical varieties [8,9]. Research highlights the extensive health benefits of honey, revealing its potential as both a therapeutic agent and nutritional powerhouse. Marta Palma et al. [10] emphasize honey's positive impact on cardiovascular health, metabolic function, mucositis, cough relief in children, and wound healing, particularly when used as a substitute for other sweeteners. Ranneh et al. [11] explore honey's anti-inflammatory

properties, focusing on its polyphenols and flavonoids that combat chronic diseases. Leoni et al. [12] examine the diversity of honey, showcasing its importance in specific ecosystems and advocating for precise analytical techniques. Ahmed et al. [13], through systematic review and meta-analysis, confirm honey's role in improving glycemic control and lipid levels, especially when integrated into a healthy diet, while highlighting the necessity of considering floral source and processing methods for optimal health outcomes.

This study pioneers a comprehensive evaluation of physical parameters and antioxidant capacities in honey samples sourced from eastern Morocco, injecting fresh perspectives into the field. Integrating molecular docking analysis was used alongside Density Functional Theory (DFT), a powerful and widely used tool in chemistry and physics to study and predict the properties of complex electronic systems, particularly in exploring honey's antioxidant potential [14]. Eastern Morocco's diverse ecological landscape likely influences the unique characteristics of its honey production, shaping its distinct chemical composition and flavor profile. Exploring the botanical diversity and chemical makeup of Eastern Moroccan honey unveils its exceptional nutritional and medicinal properties, setting it apart from honey produced elsewhere. Understanding traditional beekeeping practices in eastern Morocco provides valuable cultural context and historical insight into the region's honey production legacy. Overall, studying honey from eastern Morocco promises to uncover novel qualities and merits, enriching our understanding of honey diversity and its manifold applications.

Employing molecular docking analysis with honey compounds and cytochrome c peroxidase aims to uncover honey's antioxidant mechanisms and identify bioactive compounds. This approach aids in understanding how honey interacts with the enzyme, facilitating comparative analyses between different varieties to discern variations in antioxidant potential and contribute to quality control efforts by authenticating genuine products and detecting adulteration. These insights can guide stakeholders in the food and healthcare sectors, informing decisions pertaining to product development, quality assurance, and industry strategies [15]. Furthermore, identifying specific compounds that contribute to honey's antioxidant activity paves the way for future research focused on leveraging these properties for therapeutic purposes [16].

2. Materials and Methods

2.1. Honey Samples

This study focused on analyzing 35 honey samples obtained directly from beekeepers in eastern Morocco. These samples included a variety of types such as jujube, multifloral, citrus, eucalyptus, thyme, carob, and rosemary honeys. Collected between February and July of 2021–2022, all samples were stored in sealed plastic containers at room temperature (22–24 °C) until they were analyzed.

2.2. Physicochemical Analysis

A Kyoto Titrator was employed to measure the pH and free acidity of the honey samples. The pH was determined using a 10% (*w/v*) aqueous solution, where 2.5 g of honey was dissolved in 25 mL of Milli-Q water in a 50 mL beaker, stirred until completely dissolved. Free acidity was measured by identifying the inflection point of the neutralizing curve of the honey solution with 0.05 N sodium hydroxide (NaOH). The moisture content was assessed using a refractometric method at 20 °C, following the harmonized method established by the International Honey Commission (IHC) [17,18]. This analysis was performed in duplicate with an Abbe Refractometer ATAGO RX-5000 (Tokyo, Japan). Electrical conductivity was measured at 20 °C in honey solutions prepared with Milli-Q water using a WTW InoLab Level 1 conductivity meter (Haaksbergen, The Netherlands), following the IHC method. The protein content was determined using the Kjeldahl method [19], which involved mineralizing the nitrogenous matter with concentrated sulfuric acid and a catalyst under heat, liberating ammonia, which was then distilled into a boric acid solution and quantified. The protein level was calculated by multiplying the nitrogen content by 6.25.

Hydroxymethylfurfural (HMF) concentrations were determined using an HPLC method based on the IHC protocol [20]. A 5 g honey sample was dissolved in approximately 25 mL of Milli-Q water, clarified with potassium hexacyanoferrate (II) and zinc acetate dihydrate from (Sigma Aldrich, Burlington, MA, USA) solutions, made up to 50 mL with Milli-Q water, and centrifuged before HPLC analysis. The HPLC system included an Agilent 1200 with various components and a ZORBAX Eclipse XDB-C18 reverse phase column (Supelco, Bellefonte, PA, USA). For diastase activity measurement, 1 g of honey was dissolved in 15 mL of Milli-Q water and 5 mL of acetate buffer solution (pH 5.2), diluted to 100 mL. The reaction involved incubating the solution with a PHADEBAS tablet at 40 °C, stopping the reaction with NaOH, filtering, and measuring the absorbance at 620 nm using an Ultrospec spectrophotometer. Diastase activity was expressed in Gothe units using the formula ($DA = -4.37 \times Abs + 31.38 \times Abs + 0.03$), where DA is the diastase activity and Abs is the absorbance of the final solution at 620 nm. To ensure accuracy, each sample was analyzed in triplicate. All chemicals used in this study were obtained from Sigma-Aldrich, with a purity of 99% or higher. The water used was bidistilled.

2.3. Total Phenolics

The phenolic concentration in the honey samples was determined using a modified Folin–Ciocalteu spectrophotometric method [21]. A mixture was prepared by combining 1 mL of honey with 1 mL of Folin–Ciocalteu reagent. After a 3 min interval, 1 mL of a 10% Na₂CO₃ solution was added, and the mixture was diluted to 10 mL with distilled water. The reaction was protected from light for 90 min. Absorbance was measured at 725 nm using a UV-1650 Shimadzu spectrophotometer. Gallic acid standards (20, 40, 60, 80, and 100 µg/mL) were used to establish a calibration curve. Measurements were performed in triplicate, and the results, presented as mean ± standard deviation, were expressed as mg of gallic acid equivalents (GAEs) per kg of honey. The total polyphenol content, calculated using the Folin–Ciocalteu method, followed the equation ($Abs = 0.022 \times [GAE] + 0.003$), with a coefficient of determination of 0.999.

2.4. Total Flavonoids

The total flavonoid content of each honey sample was determined using the colorimetric method developed by Berger et al. [21]. In this procedure, 1 mL of honey was mixed with 4 mL of distilled water. Initially, 0.3 mL of 5% NaNO₂ solution was added, followed by 0.3 mL of 10% AlCl₃ solution after five minutes. Six minutes later, 2 mL of 1 M NaOH was added, and the volume was adjusted to 10 mL with an additional 2.4 mL of distilled water. The mixture was vigorously shaken, and absorbance was measured at 510 nm. A calibration curve was established using a standard catechin solution (20, 40, 60, 80, and 100 µg/mL). Results were expressed as mg catechin equivalents (CEQs) per kg of honey. Flavonoid content was also expressed as mg quercetin equivalents (QEs) per gram of extract, using the standard curve equation for quercetin ($Abs = 0.012 \times [QE] + 0.002$), with a coefficient of determination of 0.998.

2.5. DPPH Free Radical-Scavenging Activity

The antioxidant capabilities of each honey sample were examined by assessing the free radical-scavenging activity of the DPPH radical, following the procedure outlined by Ferreira et al. [22]. To accomplish this, a methanolic solution with DPPH radicals (0.024 mg/mL, 2.7 mL) was combined with honey (0.5 mL). After mixing vigorously, the solution was kept in the dark for 15 min. The decrease in the 2,2-diphenyl-1-picrylhydrazyl (DPPH) radical was measured checking the absorbance at 517 nm, following the method described by Hatano et al. [23]. Butylated hydroxytoluene (BHT) was used as a standard reference. The radical scavenging activity (RSA) was calculated as the percentage of DPPH discoloration using the formula:

$$\%RSA = ((A_{DPPH} - A_S) / A_{DPPH}) \times 100 \quad (1)$$

where A_S is the absorbance of the solution with the honey, and A_{DPPH} is the absorbance of the DPPH solution alone.

2.6. HPLC and GC-MS Analysis

An HPLC Agilent 1200 system with an LC-20AT quaternary pump, DGU-20A5 degasser, SIL-20AC auto-sampler, SPD20A diode array detector, and CTO-20AC column oven was used. The system was controlled by Shimadzu Client/Server software, version 7.3, from Shimadzu Corporation (Tokyo, Japan). The column used was a ZORBAX Eclipse XDB-C18 reverse-phase stainless steel column (Supelco, Bellefonte, PA, USA) with dimensions of 150 mm \times 4.6 mm i.d. and a film thickness of 5 μ m, operated at 30 $^{\circ}$ C along with a C18 guard column. The mobile phase consisted of water and methanol (90:10, *v/v*), with a flow rate of 0.7 mL/min and an injection volume of 10 μ L. Injections were performed with a needle wash. Serial standard solutions of HMF (1–50 mg/L) were prepared in Milli-Q water. The calibration curves and chromatograms used to determine the HMF content in the seven honey samples are shown in Figures S1–S8.

For GC-MS measurements, an Agilent 7890A GC system (Santa Clara, CA, USA) was used alongside a 5975C MS system and an FID detector, all operating synchronously. The column employed was the BPx90 brand (London, UK), with dimensions of 100 mm \times 0.25 mm \times 0.25 μ m. Helium gas served as the carrier gas, maintaining a flow rate of 1 mL/min. The temperature of the samples was increased by 5 $^{\circ}$ C per minute under the chromatographic conditions, starting from 120 $^{\circ}$ C and reaching 254 $^{\circ}$ C, where it was held for approximately 16 min. For the GC-MS measurement, a portion of the filtered clear solution was processed as follows: 100 μ L of the sample was mixed with 10 mL of hexane and vortexed. Then, 100 μ L of 2 N KOH was added to the resulting solution and vortexed again. The solution was centrifuged at 4500 rpm for 10 min. Finally, the clear portion of the organic phase from the centrifuged tubes was placed into the GC-MS device, ready for measurement. The results obtained from the GC-MS analysis, based on the existing database of the seven honeys studied, are presented in Table S1.

2.7. Molecular Docking Study

Based on the results of the GC-MS analysis, the most abundant compounds (over 14%) in the volatile fractions of the honey samples were selected for molecular docking calculations. The aim was to identify compounds potentially responsible for the observed antioxidant activity. The 3D structures of select biocompounds, such as benzaldehyde, phenylacetaldehyde, phenylacetic acid, thymol, ethyl phenylacetate, 1-octene, hotrienol, and ascorbic acid, were used in this study. Crystal structures of cytochrome c peroxidase in a complex with ascorbic acid, with a resolution of 2.01 Å [24], were downloaded from the RCSB protein database (www.rcsb.org) to serve as the enzyme receptor in this study. Virtual screening was performed using PyRx 8.0 software. A 30 \times 30 \times 30-point grid, centered on the coordinates -15.25 , -0.61 , and 5.72 , was used to encompass the receptor's active site pocket. The preparation of the target receptor and visualization of interactions in a 2D format of ligand–receptor complexes were carried out using BIOVIA Discovery Studio Visualizer 2020. The binding affinity of each compound to the target receptor was assessed in terms of the Gibbs free energy of binding (ΔG), calculated using PyRx 8.0 software.

2.8. DFT Calculations

DFT calculations involve the selection of an exchange–correlation functional, configuration of system parameters, and iterative solution of the Kohn–Sham equations for electron density until convergence is achieved. The accuracy of outcomes hinges on the chosen functional and computational parameters, validated against experimental data, offering insights into electronic structures and material characteristics. Utilizing the DFT approach, structural configurations of ethyl phenylacetate and thymol were refined. The optimization procedure employed a 6-31G(d,p) basis set at the B3LYP level of theory within the Gaussian 09 software suite [25]. A visual representation of the results, including optimized

geometries, HOMO-LUMO shapes, and MEP maps, was facilitated through the graphical interface of GaussView 6 [26].

3. Results

3.1. Physicochemical Properties

The physicochemical analysis results detailed in Table 1 illustrate that the average values of the parameters investigated in the honey samples conform to the limits established by the European Commission Regulation of 2002. The eastern Morocco honey samples under scrutiny demonstrated an acidic nature, with pH values ranging from 3.79 to 4.94 (Table 1). These pH values closely resemble those previously documented for honey samples from various regions, including India, Brazil, Spain, and Turkey, which ranged from 3.49 to 4.70 [27]. Elevated acidity levels in honey indicate the potential fermentation of sugars into organic acids. However, none of the examined samples exceeded the permissible limit, indicating the freshness of all honey samples. The free acidity of all eight samples fell within the permitted range of no more than 50 milliequiv acid/kg [17,28]. In this study, the free acidity of the honey samples ranged from 5.77 ± 1.77 to 15.07 ± 7.89 milliequiv acid/kg in Jujube and Multifloral honeys, respectively (Table 1), consistent with findings from Turkish honey [29]. Carob honey displayed a notably high protein content (0.42%) compared to the average protein content in other analyzed honeys, which typically ranges around 0.26% with a maximum of 0.83% [30]. Moisture content significantly influences honey's resistance to fermentation and granulation during storage [31]. In this study, all samples fell within an acceptable moisture range, ranging from 15.39% to 19.74%, similar to findings in Portuguese honey (13.6% to 19.2%) [32], Turkish honey (13.2% to 19.2%), and Algerian honey (14.6% to 19%) [33]. The low moisture content observed in the examined honey samples suggests good quality and suitability for storage.

Table 1. Physicochemical parameters of honey from different flora of eastern Morocco.

Flora	pH	Free Acidity (meq/kg)	Moisture (%)	Diastase (Gothe)	Proteins (%)	HMF mg/kg	ABS ₄₅₀ (mAU; 50 w/v)
Jujube	4.94 ± 0.68^b	5.77 ± 1.77^c	15.39 ± 0.64^b	21.17 ± 2.33^c	0.34 ± 0.05^a	3.98 ± 4.67^d	675.12 ± 2.12^c
Multifloral	4.30 ± 0.2^b	15.07 ± 7.89^d	17.17 ± 1.63^c	17.82 ± 6.45^d	0.40 ± 0.14^b	10.02 ± 4.66^c	795.15 ± 3.57^c
Citrus	3.79 ± 0.10^a	14.97 ± 2.89^c	17.76 ± 1.43^c	12.71 ± 1.60^c	0.31 ± 0.02^a	27.15 ± 8.73^d	560.03 ± 0.74^b
Eucalyptus	4.22 ± 0.59^b	13.68 ± 4.93^c	19.37 ± 2.17^c	11.96 ± 9.20^d	0.30 ± 0.01^a	38.55 ± 5.60^d	734.60 ± 2.82^c
Thyme	4.36 ± 0.03^a	12.04 ± 0.94^b	16.85 ± 0.36^b	18.72 ± 2.48^c	0.39 ± 0.01^a	10.16 ± 3.63^c	318.02 ± 0.72^b
Carob	4.20 ± 0.44^b	14.10 ± 1.71^c	15.59 ± 1.23^c	15.28 ± 8.37^d	0.42 ± 0.1^a	3.34 ± 3.36^c	847.10 ± 1.46^c
Rosemary	3.68 ± 0.1^a	6.01 ± 1.33^c	17.92 ± 1.98^c	6.98 ± 2.36^c	0.22 ± 0.01^a	15.14 ± 4.86^c	198.01 ± 2.36^c
Range	3.79–4.94	5.77–15.07	15.39–19.37	6.98–21.17	0.22–0.42	3.98–38.55	198–847
Mean	4.21 ± 0.4	11.66 ± 2.60	17.15 ± 0.31	14.94 ± 1.40	0.41 ± 0.02	15.47 ± 4.10	589.65 ± 1.05

Results are expressed as mean \pm SD (n = 3). Significant differences in the same row are shown by different letters (a–d) for varieties ($p \leq 0.05$).

Diastase activity and HMF content serve as key indicators of honey freshness [34]. The average diastase activity observed in all samples was 14.70, with three samples (rosemary honey) surpassing the acceptable limit, likely due to excessive heat treatment during processing, which diminishes the diastase enzyme level. HMF levels in the samples ranged from 3.98 to 38.55 mg/kg (Table 1), all falling within the recommended range set by the *Codex Alimentarius* [17,27]. The color intensity of honey often reflects its origin and composition [34,35]. In the analyzed honey samples, the color intensity (ABS₄₅₀) ranged from 198 to 847 mAU (Table 1), with carob honey showing the highest intensity of 847 mAU, suggesting a high antioxidant potential. In comparison, ABS₄₅₀ values in honey samples from other countries varied significantly, with values ranging from 25 to 3413 mAU in Italian honey, 724 to 1188 mAU in Algerian honey, 70 to 495 mAU in Slovenian honey, and 524 to 1678 mAU in Indian honey [36].

3.2. Total Polyphenol Content

The polyphenol content of various honeys was assessed using the modified Folin–Ciocalteu assay, which detects phenol and polyphenol entities, as well as other compounds like ascorbic acid and vitamin E [37]. Table 2 presents the total polyphenol content for seven types of honey, indicating varying levels depending on the flower source in the following order: carob honey > multifloral honey > eucalyptus honey > jujube honey > citrus honey > thyme honey. Carob honey showed the highest concentration of polyphenols at 720.16 mg gallic acid/kg, underscoring its significant polyphenol presence. Generally, darker honeys tend to contain higher levels of polyphenolic compounds compared to lighter varieties, influencing their deeper amber hues [38]. Variations in polyphenol content among honey samples may be attributed to natural differences in composition (such as sugar, mineral, and water content), diverse geographical origins, and the specific floral sources of nectar.

Table 2. Total phenolic and flavonoid contents and antioxidant properties of seven eastern Morocco honeys.

Honey	Total Polyphenols (mg gallic acid/kg)	Flavonoids (mg catechin/kg)	DPPH Radical-Scavenging Activity (%)
Jujube	579.99 ± 0.8 ^a	50.80 ± 1.5 ^b	57.57 ± 0.7 ^a
Multifloral	643.33 ± 1.3 ^b	70.67 ± 0.5 ^a	60.39 ± 1.1 ^b
Citrus	493.33 ± 0.4 ^a	40.30 ± 1.7 ^c	45.47 ± 1.6 ^c
Eucalyptus	608.45 ± 1.1 ^b	60.90 ± 0.3 ^a	53.33 ± 0.8 ^a
Thyme	454.99 ± 1.2 ^b	50.30 ± 0.5 ^a	43.33 ± 0.9 ^a
Carob	720.16 ± 0.5 ^a	90.50 ± 1.1 ^b	63.50 ± 1.3 ^a
Rosemary	266.66 ± 0.9 ^a	25.01 ± 0.9 ^a	36.15 ± 1.5 ^b

Results are expressed as mean ± SD (n = 3). Significant differences in the same row are shown by different letters (a–c) for varieties ($p \leq 0.05$).

3.3. Flavonoid Content

Flavonoids, identified as low-molecular-weight phenolic compounds, play a crucial role in shaping both the aroma and flavonoid potential of honey. The total content of flavonoids in the tested honey samples ranged from 25 to 90.5 mg catechin/kg (Table 2). Similar to the phenolic content, carob honey exhibited the highest flavonoid content (90.5 mg/kg) among all types of honey examined, followed by multifloral honey with a concentration of 70.67 mg/kg. These concentrations exceed those found in Turkish honey [39] and Malaysian honey, which range from 4.80 to 22.80 mg/kg and 11.52 to 25.31 mg/kg, respectively [40], indicating that honey from eastern Morocco possesses higher flavonoid potential. Consequently, honey with elevated flavonoid concentrations is desirable for its purported health-promoting properties.

3.4. Antioxidant Activity

The DPPH assay, utilizing a stable nitrogen-centered radical, is widely employed to assess the antioxidant capabilities of various samples. The presence of an unpaired electron in DPPH results in absorption peaks at 517 nm, imparting a purple coloration. Upon interacting with hydrogen from free radical-scavenging antioxidants, DPPH undergoes a color shift from purple to yellow, indicating reduction. In this study, honeys from eastern Morocco were evaluated for their DPPH radical-scavenging activities, revealing significant antioxidant potential (Table 2). Across concentrations ranging from 10 to 120 mg/mL, honey samples demonstrated varying degrees of DPPH radical inhibition, ranging from 36.15% to 63.5%. Notably, carob honey exhibited the highest inhibition at 120 mg/mL (63.5%), underscoring its exceptional antioxidant capacity. The ranking of scavenging efficacy among the honey samples was as follows: carob honey > multifloral honey > jujube honey > eucalyptus honey > citrus honey > thyme honey. These findings highlight the superior antioxidant properties of eastern Moroccan honey, surpassing those reported for Malaysian and Indian honey varieties in comparable studies [39,41].

3.5. Correlation Amongst Biochemical Parameters and Antioxidant Properties

The correlation matrix (Table 3) provides insights into the relationships among key parameters measured in honeys from eastern Morocco. Phenolics exhibit strong positive correlations with flavonoids ($r = 0.925, p < 0.01$), DPPH radical-scavenging activity (RSA) ($r = 0.961, p < 0.01$), and ABS_{450} ($r = 0.963, p < 0.01$), indicating that higher levels of phenolics correspond to increased flavonoid content and enhanced antioxidant capacity, as measured by both $DPPH_{RSA}$ and ABS_{450} . Similarly, flavonoids show significant positive correlations with phenolics ($r = 0.925, p < 0.01$), $DPPH_{RSA}$ ($r = 0.894, p < 0.01$), and ABS_{450} ($r = 0.839, p < 0.05$), reinforcing their role in antioxidant potential. Similar correlations were noted in previous studies on honey samples from Malaysia [35,40]. $DPPH_{RSA}$ also correlates strongly with phenolics ($r = 0.961, p < 0.01$) and ABS_{450} ($r = 0.952, p < 0.05$), indicating that higher $DPPH_{RSA}$ values are associated with greater phenolic content and ABS_{450} absorption. ABS_{450} , in turn, shows robust positive correlations with phenolics ($r = 0.963, p < 0.01$), flavonoids ($r = 0.839, p < 0.05$), and $DPPH_{RSA}$ ($r = 0.952, p < 0.05$), highlighting its alignment with phenolic and flavonoid levels and its influence on antioxidant activity. These findings collectively underscore the interdependent relationships among phenolics, flavonoids, $DPPH_{RSA}$, ABS_{450} , and protein content in eastern Moroccan honeys, elucidating their combined influence on antioxidant properties and potential health benefits.

Table 3. Correlation matrix showing the interrelation among phenolics, flavonoids, $DPPH_{RSA}$, ABS_{450} , and protein.

	Phenolics	Flavonoids	$DPPH_{RSA}$	ABS_{450}	Protein
Phenolics	1	0.925 ^a	0.961 ^a	0.963 ^a	0.763 ^b
Flavonoids	0.925 ^a	1	0.894 ^a	0.839 ^b	0.826 ^b
$DPPH_{RSA}$	0.961 ^a	0.894 ^a	1	0.952 ^b	0.721 ^c
ABS_{450}	0.963 ^a	0.839 ^b	0.952 ^b	1	0.593 ^d
Protein	0.763 ^b	0.826 ^b	0.721 ^c	0.593 ^d	1

RSA for radical-scavenging activity. ^a Correlation significant differences in the same row are shown by different letters (a–d) for varieties ($p \leq 0.05$).

3.6. Molecular Docking

The chemical profiles of various honey types exhibit distinct compositions, showcasing specific compounds that contribute to their unique characteristics. Jujube honey is notable for its high ethyl phenylacetate content (14.7%), whereas multifloral honey shows elevated levels of benzaldehyde (12.9%) and phenylacetaldehyde (15.4%). Citrus honey stands out with significant linalool oxide (11.3%) and moderate benzaldehyde content (6.3%), while eucalyptus honey is characterized by a dominance of octene (33.9%) and phenylacetic acid (17.6%). Thyme honey features substantial thymol (16.4%) and benzaldehyde (14.4%), whereas carob honey exhibits a notable presence of phenylacetaldehyde (27.12%). Rosemary honey, with benzaldehyde (9.9%) as its major compound and minimal phenylacetaldehyde (1.2%), provides a contrast in its chemical profile. These variations underline how different floral sources influence the composition and sensory attributes of honey. Table S1 lists the compounds identified by the GC-MS analysis in the different honeys, while the ten most important compounds in the chemical composition of the honey samples are shown in Table 4.

3.7. Molecular Docking

In the realm of molecular research, molecular docking stands out as a powerful computational tool esteemed for its ability to forecast and decipher potential binding interactions between molecules and specific target proteins or receptors [42,43]. These interactions unveil crucial insights into the binding mode and probable binding sites of various compounds within protein frameworks, pivotal for gauging and comprehending

their effectiveness as therapeutic agent [44]. In line with this, the primary aim of this study was to unravel a coherent rationale and pinpoint potential compounds responsible for the observed antioxidant activity in the honey samples under scrutiny. The investigation centered on a targeted docking study of the cytochrome c peroxidase protein, focusing on binding energy as a key stability indicator. The results, highlighted in Table 5, showcase ethyl phenylacetate's remarkable binding energy superiority over other compounds like thymol, phenylacetic acid, phenylacetaldehyde, and benzaldehyde. Visualized in Figure 1 are the 2D interactions within cytochrome c peroxidase's binding pocket, where lower scores signify stronger interactions.

Table 4. The most important compounds in the chemical composition of honey samples, as determined by GC-MS analysis.

Type of Honey		Jujube		Multifloral		Citrus		Eucalyptus		Thyme		Carob		Rosemary	
Compounds	RT	Pa	Area %	Pa	Area %	Pa	Area %	Pa	Area %	Pa	Area %	Pa	Area %	Pa	Area %
Phenol	38.75	99.07	4.10	99.36	4.30	98.52	1.70	82.30	0.20	-	-	99.85	2.60	99.50	12.50
2-butanol	37.95	23.49	0.10	-	-	98.82	1.80	-	-	-	-	-	-	99.74	12.60
Thymol	36.64	-	-	-	-	-	-	-	-	99.15	16.40	-	-	-	-
Ethyl phenylacetate	33.58	99.43	14.70	-	-	-	-	99.95	5.50	99.53	3.70	-	-	86.14	0.60
2-butanone	32.30	-	-	-	-	-	-	98.87	3.90	-	-	85.54	0.30	98.61	13.40
Isophorone	30.11	99.09	9.20	98.33	3.10	97.05	1.10	95.40	0.70	93.66	0.40	86.05	1.10	98.47	4.10
Linalool oxide	23.74	-	-	-	-	99.53	16.20	-	-	-	-	-	-	-	-
Phenylacetaldehyde	22.18	99.26	4.50	99.75	15.40	99.64	3.10	95.89	0.40	99.28	10.22	99.49	27.20	98.57	1.20
1-octene	18.61	-	-	-	-	-	-	99.20	33.90	-	-	-	-	-	-
Phenylacetic acid	17.23	-	-	99.42	5.80	-	-	99.95	17.60	-	-	90.22	1.20	-	-
Benzaldehyde	16.30	99.68	2.80	99.49	12.90	99.03	6.30	99.77	1.70	98.64	14.40	98.28	8.80	99.19	9.90
3-furaldehyde	9.74	99.48	3.40	99.90	4.50	98.42	2.10	99.34	9.70	93.42	1.10	90.92	8.10	98.62	2.10

Table 5. Docking findings of major compounds in the volatile fractions of the examined honey samples against cytochrome c peroxidase protein.

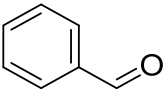
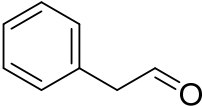
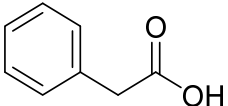
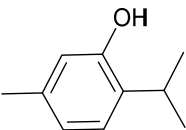
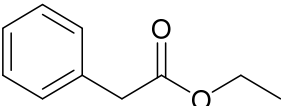
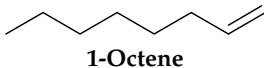
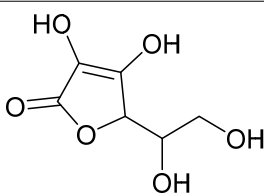
Compound	Score (kcal/mol)	Involved Receptor Residues	Distance (Å)
 Benzaldehyde	-6.2	His299/HB Trp51/HB and pi-pi Leu171/pi-alkyl Ala174/pi-alkyl	2.46 2.80 and 4.31 4.44 4.75
 Phenylacetaldehyde	-6.2	His175/HB Trp51/HB and pi-pi Leu171/pi-sigma Ala174/pi-alkyl	2.54 2.51 and 4.49 2.81 4.90
 Phenylacetic acid	-6.3	His175/UDD Trp51/HB and pi-pi Leu171/pi-sigma Ala174/pi-alkyl	1.37 2.32 and 4.54 2.82 4.90
 Thymol	-6.7	Trp51/pi-pi and pi-alkyl Leu171/alkyl Ala174/pi-alkyl and alkyl Arg48/alkyl Val47/alkyl	4.17 and 4.47 3.99 3.54 and 4.01 3.86 4.54
 Ethyl phenylacetate	-6.9	His175/HB Trp51/HB; pi-pi Leu171/pi-sigma Ala174/alkyl Arg48/alkyl	2.19 2.75 and 4.49 2.74 4.46 3.68

Table 5. Cont.

Compound	Score (kcal/mol)	Involved Receptor Residues	Distance (Å)
 1-Octene	−5.3	Trp51/pi-alkyl Leu171/alkyl Ala174/alkyl Arg48/alkyl Val47/alkyl Phe158/pi-alkyl Phe266/pi-alkyl	4.39; 4.39 and 4.08 4.47 and 4.88 3.84 4.22 4.54 4.67 3.87
 Ascorbic Acid	−5.8	Lys179/HB Asp37/HB Arg184/HB Pro44/CHB Val45/CHB Arg48/CHB Gly178/CHB	2.03 and 2.49 2.31 2.34 2.82 2.45 2.96 2.41 and 2.67

HB: Hydrogen bond; VDW: Van der Waals forces; CHB: Carbon hydrogen bond; UDD: Unfavorable donor–donor.

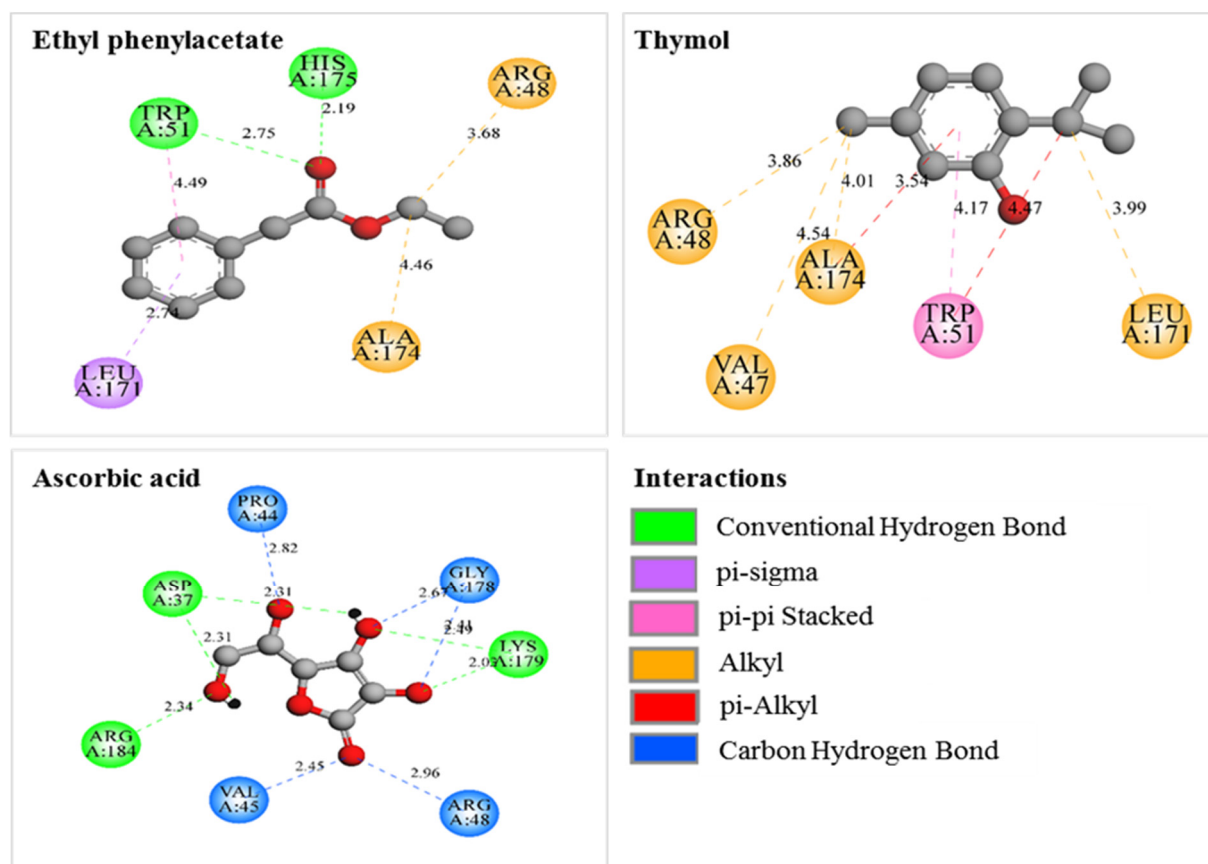


Figure 1. Two-dimensional plots of the best docked poses of the studied compounds into the cytochrome c peroxidase active pocket.

In silico results revealed that the compounds exhibited higher binding scores than ascorbic acid (−5.8 kcal/mol), except for 1-octene (−5.3 kcal/mol). Notably, ethyl phenylacetate displayed the highest binding energy with a score of −6.9 kcal/mol, followed closely by thymol (−6.7 kcal/mol), phenylacetic acid (−6.3 kcal/mol), phenylacetaldehyde (−6.2 kcal/mol), and benzaldehyde (−6.2 kcal/mol). These findings suggest the stabilization of these compounds within the binding pocket of cytochrome c peroxidase. Studies

conducted by Che Muhammad K.H.I. et al. [45] demonstrated promising findings regarding the binding affinities of SDC and FMN to ACE-2 receptors, exhibiting robust binding energies of -9.719 and -9.473 kcal/mol, respectively. Meanwhile, Zhenchun Sun et al. [46] delved into the aromatic compounds present in Zunyi black tea, utilizing GC-MS-O and molecular docking techniques. Their research identified honey-like aromatic compounds interacting with specific receptors, showcasing varying binding energies ranging from -4.34 to -5.33 kcal/mol across five receptors. Furthermore, Abdulrahman S. et al.'s [47] investigation into Saudi Sidr honey unveiled significant antioxidant activity, evidenced by IC₅₀ values of 5.41 mg/mL for ABTS and 7.70 mg/mL for DPPH testing, suggesting its therapeutic potential.

A visualization of the intermolecular interaction modes between the investigated compounds and their enzyme target was generated to gain further insights into the interaction mechanisms. Interestingly, all compounds exhibited interactions with three crucial amino acids, namely Trp51, Leu171, and Ala174, as outlined in Table 5. Besides these primary interactions, the compounds also formed additional binding interactions with various other amino acids. For instance, benzaldehyde interacted with His299, phenylacetaldehyde, ethyl phenylacetate, and phenylacetic acid interacted with His175, and thymol, ethyl phenylacetate, and 1-octene interacted with Arg48. Additionally, 1-octene interacted with the Val47, Phe158, and Phe266 amino acids. These supplementary interactions played a crucial role in stabilizing the ligand–enzyme complex formed, potentially explaining the lower binding scores of the studied compounds compared to ascorbic acid.

The 2D interaction plots presented in Figure 1 were generated by selecting the optimal binding poses of ethyl phenylacetate, thymol, and ascorbic acid. Ethyl phenylacetate demonstrated favorable interactions within the active pocket, forming a hydrogen bond with His175 at an average length of 2.19 Å. It also engaged in a hydrogen bond and a pi–pi interaction with Trp51 at distances of 2.75 and 4.49 Å, respectively. Furthermore, it formed a pi–sigma bond with Leu171 at 2.74 Å and two alkyl bonds with Ala174 and Arg48 at distances of 4.46 and 3.68 Å, respectively. Thymol's binding within the active pocket involved a pi–pi interaction and a pi–alkyl interaction with Trp51 at distances of 4.17 and 4.47 Å, respectively. It also formed an alkyl bond with Leu171 at 3.99 Å and pi–alkyl and alkyl interactions with Ala174 at distances of 3.54 and 4.01 Å, respectively. Additionally, it engaged in alkyl bonds with Arg48 and Val47 at distances of 3.86 and 4.54 Å, respectively. Ascorbic acid interacted within the protein's active pocket through four hydrogen bonds, with Lys179, Asp37, and Arg184 residues at distances of 2.03, 2.49, 2.31, and 2.34 Å, respectively. Furthermore, it formed five carbon–hydrogen bonds with the amino acids Pro44, Val45, Arg48, and Gly178 at distances of 2.82, 2.45, 2.96, 2.41, and 2.67 Å, respectively.

The molecular docking analysis unequivocally reveals the potent inhibitory effects of the tested compounds on the cytochrome c peroxidase enzyme compared to ascorbic acid. These compounds demonstrate significant interactions with crucial residues within the active pocket, primarily through hydrogen and electrostatic interactions. Regarding the interpretation of the observed antioxidant activities in honey samples, this study posits that these samples harbor compounds that, either individually or synergistically, bolster their antioxidant potential. Notably, the presence of ethyl phenylacetate, phenylacetic acid, benzaldehyde, and phenylacetaldehyde in substantial proportions appears to positively influence the antioxidant potential. However, despite its high docking score and exclusive presence in thyme honey, thymol alone cannot entirely account for the observed low antioxidant activity, likely due to its abundance and specific mechanism of action.

3.8. DFT Study

DFT calculations were performed for the most-binding molecules, specifically ethyl phenylacetate and thymol, within the active pocket of the cytochrome c peroxidase protein. These calculations were conducted at the DFT/B3LYP/6–31G(d,p) level.

3.8.1. HOMO-LUMO Analysis

The assessment of a molecule's electronic properties through frontier molecular orbitals (FMOs), specifically the Highest Occupied Molecular Orbital (HOMO) and Lowest Unoccupied Molecular Orbital (LUMO), provides valuable insights into its reactivity and stability across various reactions. The HOMO signifies the molecule's capacity to donate electrons, while the LUMO indicates its ability to receive electrons. Furthermore, the energy gap ($\Delta E = E_{\text{LUMO}} - E_{\text{HOMO}}$) serves as a crucial parameter for measuring charge transfer within the molecule and its kinetic stability, often employed in interpreting biological activity [48]. Generally, molecules with a larger energy gap tend to display lower chemical reactivity and higher kinetic stability, whereas those with a smaller ΔE are more reactive but less stable [49].

Examining the HOMO and LUMO energies of ethyl phenylacetate and thymol yields comprehensive global reactivity descriptors. Ethyl phenylacetate showcases an E_{HOMO} of -6.555 eV and E_{LUMO} of -0.206 eV, while thymol presents an E_{HOMO} of -5.722 eV and E_{LUMO} of 0.171 eV. Consequently, the energy gap values ($\Delta E = E_{\text{LUMO}} - E_{\text{HOMO}}$) for ethyl phenylacetate and thymol are calculated as 6.349 eV and 5.893 eV, respectively, indicating the higher stability of ethyl phenylacetate compared to thymol. Notably, the enhanced stability of ethyl phenylacetate is significantly influenced by the LUMO energy level, contributing to its strong affinity for the cytochrome c peroxidase protein observed in the docking section. However, it is crucial to recognize that the correlation between LUMO energy and biological activity is not the sole determinant. Exploring additional factors such as the shape and location of molecular orbitals, influenced by the presence or absence of electron-donating or -withdrawing groups, is essential. Investigations have revealed that the location and energy of LUMO, along with other characteristics of molecular orbitals, collectively impact biological activity [50].

The graphical representation of frontier molecular orbital shapes for both molecules (Figure 2) illustrates that in ethyl phenylacetate, the occupied orbital (HOMO) and empty LUMO orbital are localized over the entire molecule, except for the ethyl group. Conversely, for thymol, the electron density of HOMO is distributed throughout the entire molecule, while the empty LUMO orbital is primarily concentrated on the benzene ring.

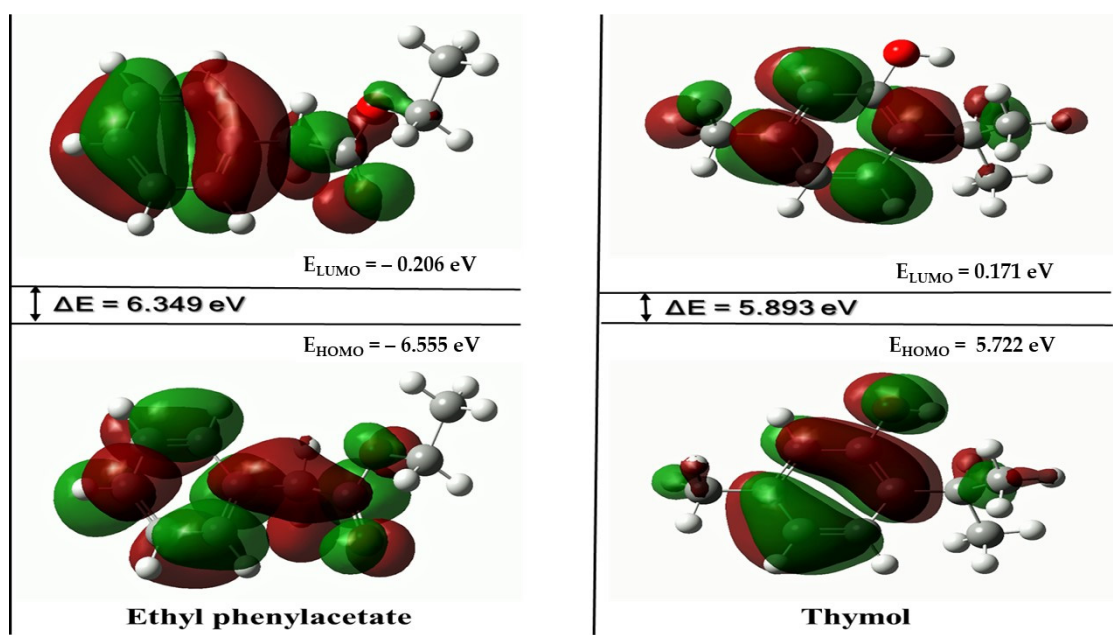


Figure 2. HOMO and LUMO plots of ethyl phenylacetate and thymol. Positive and negative phases are displayed in red and green colors, respectively.

3.8.2. Global Reactivity Descriptors

To comprehensively understand the structural properties of the compounds under investigation, a variety of quantum chemical descriptors derived from Koopmans' theorem were computed. These parameters, which include chemical hardness (η), softness (σ), electronegativity (χ), chemical potential (μ), and global electrophilicity index (ω), were determined using appropriate formulas based on the HOMO and LUMO energies (Table 6) [51,52]. These descriptors play a critical role in evaluating the stability and reactivity of a species. They provide insights into the molecule's resistance to deformation or polarization of electron density, its ability to attract electrons, the propensity of an electron to escape from the molecule, and the species's capability to accept electrons. Consequently, compounds with high values of chemical hardness are considered stable with low reactivity, while those with elevated values of softness, electronegativity, chemical potential, and electrophilicity are considered less stable and therefore exhibit greater reactivity [53].

Table 6. Calculated quantum chemical parameters for ethyl phenylacetate and thymol.

Chemical Reactivity Indices (eV)	Ethyl Phenylacetate	Thymol
E_{HOMO}	−6.555	−5.722
E_{LUMO}	−0.206	0.171
$\Delta E = E_{\text{LUMO}} - E_{\text{HOMO}}$	6.349	5.893
Chemical hardness ($\eta = (E_{\text{LUMO}} - E_{\text{HOMO}})/2$)	3.174	2.893
Softness ($\sigma = 1/\eta$)	0.315	0.345
Electronegativity ($\chi = -(E_{\text{LUMO}} + E_{\text{HOMO}})/2$)	3.380	2.775
Chemical potential ($\mu = -\chi$)	−3.380	−2.775
Electrophilicity index ($\omega = \mu^2/2\eta$)	2.274	1.330

The analysis of these parameters clearly indicates a significant level of stability for both molecules, with ethyl phenylacetate holding a slight advantage. Ethyl phenylacetate exhibits a high resistance to changes in its electronic distribution compared to thymol, as evidenced by its chemical hardness value of 3.174 eV (in contrast to thymol's 2.893 eV). The chemical potentials for ethyl phenylacetate and thymol were calculated as −3.380 eV and −2.775 eV, respectively, indicating that both molecules act as good electron donors. Furthermore, the calculated electrophilicity values classify ethyl phenylacetate as a strong electrophile with a value of 2.274 eV, while thymol is categorized as a moderate electrophile with a value of 1.330 eV (based on the following scale: weak electrophile: $\omega < 0.8$ eV; moderate electrophile: $0.8 < \omega < 1.5$ eV; strong electrophile: $\omega > 1.5$ eV [54]). In general, the computed descriptors suggest that both molecules are stable compounds, consistent with the findings from molecular docking studies. Importantly, compounds exhibiting high stability often correspond to the most stable ligand–protein complexes [55].

3.8.3. Molecular Electrostatic Potential

The investigation of molecular electrostatic potential (MEP) [56] was conducted to identify and predict reactive sites for nucleophilic and electrophilic attacks. MEP serves as a powerful tool for understanding the interaction between a molecular system and its surroundings, as well as for studying biological recognition processes and hydrogen-bonding interactions. In the realm of molecular docking and drug design, MEP assists in identifying optimal binding sites and designing new compounds with desired properties [57].

MEP plots are generated by mapping electrostatic potential onto the isoelectron density surface of each molecule, revealing the distribution of electronic charge across the entire structure. Different colors represent various electrostatic potential values on the surface, with red indicating areas of high electron density and blue highlighting regions with minimal electron concentration. Negative regions (red, orange, and yellow) are associated

with electrophilic reactivity, while positive regions correspond to nucleophilic reactivity (blue and sky blue).

As illustrated in Figure 3, the MEP values of ethyl phenylacetate span from -1.451 to 1.451 eV. The most negative charge (red) is concentrated on the two oxygen atoms of the acetate moiety, indicating potential sites for electrophilic attacks. This observation corroborates with the docking results, which identified these oxygen atoms for hydrogen bonding with amino acid residues His175 and Trp51. Conversely, positive regions are distributed across the benzene ring and ethyl group, interacting with amino acid residues Leu171, Ala174, and Arg48. For thymol, the MEP values range from -1.692 to 1.692 eV, with red regions primarily observed on the oxygen atom and benzene ring, while blue regions are evident around the hydrogen atom of the OH group and methyl groups. The notable correlation between docking results and generated MEP plots underscores the validity of our findings and emphasizes the importance of considering both aspects in this analysis.

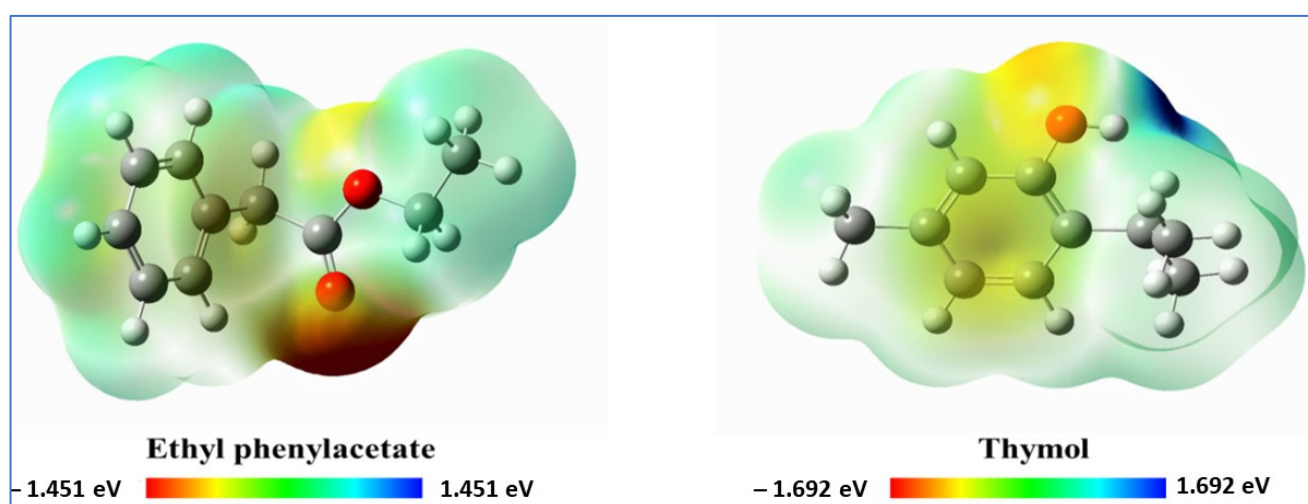


Figure 3. MEP maps of the studied compounds.

4. Conclusions

This study marks a pioneering effort in thoroughly investigating the physicochemical and antioxidant characteristics of honeys originating from eastern Morocco. This research unveiled the notable antioxidant capacity in these honey samples, highlighted by their high levels of phenolic compounds, flavonoids, and proteins. Among the various honey types examined, carob honey stood out, displaying the highest concentrations of phenolic compounds and flavonoids, coupled with intense coloration, indicating superior antioxidant potential. Furthermore, this study revealed strong positive correlations between different antioxidant markers, emphasizing the multifaceted nature of honey's antioxidant properties. These correlations suggest that the observed antioxidant effects in eastern Moroccan honeys may arise from a combination of phenolic compounds, ascorbic acid, flavonoids, and color pigments. Intriguingly, the application of molecular docking simulations to the cytochrome c peroxidase enzyme uncovered fascinating bioactive compounds within the volatile fractions of the tested honey samples. These compounds displayed a remarkable affinity for binding within the active site of the target receptor. Additionally, our findings demonstrated a significant correlation between docking results and DFT calculations, offering further insights into the antioxidant potential of the honey samples under investigation. Finally, this study highlights the rich antioxidant profile of honeys from eastern Morocco and sheds light on the underlying molecular mechanisms driving their beneficial effects. These findings not only contribute to our understanding of honey's therapeutic properties but also pave the way for the development of novel antioxidant-rich products with potential health benefits.

Supplementary Materials: The following supporting information can be downloaded at: <https://www.mdpi.com/article/10.3390/agriculture14091540/s1>, Table S1. Chemical composition of honey samples determined by GC-MS analysis (where (Pa) denotes the probability of the assignment, (RT) represents the retention time, and (-) indicates unidentified compounds), based solely on the GC-MS library; Figure S1. Calibration curve of HMF (RT = 8.736 min; Wavelength 285 nm); Figure S2. Chromatogram of Jujube honey; Figure S3. Chromatogram of Multifloral honey; Figure S4. Chromatogram of Citrus honey; Figure S5. Chromatogram of Eucalyptus honey, Figure S6. Chromatogram of Thyme honey; Figure S7. Chromatogram of Carob honey; Figure S8. Chromatogram of Rosemary honey.

Author Contributions: Conceptualization, A.A. and H.E.F.; methodology, A.A. and H.E.F.; validation, H.E.F. and A.T.; investigation, A.E.B., E.B., M.S. and H.E.F.; resources, H.E.F.; writing—original draft preparation, H.E.F. and A.A.; writing—review and editing, M.-L.F., E.B. and H.E.F.; supervision, H.E.F. and A.T. All authors have read and agreed to the published version of the manuscript.

Funding: This research received no external funding.

Data Availability Statement: The data presented in this study are available in the Supplementary Materials.

Acknowledgments: This work is the result of the valorization of the bio-resources in the Laboratory of Environment and Applied Chemistry (LCAE), Team: Physical Chemistry of the Natural Resources and Processes, Department of Chemistry, Faculty of Science, Oujda, Morocco. The authors are thankful to the director of the platform analysis at the Faculty of Science Oujda for facilitating the many different analyses.

Conflicts of Interest: The authors declare no conflicts of interest.

References

- Gheldof, N.; Engeseth, N.J. Antioxidant capacity of honeys from various floral sources based on the determination of oxygen radical absorbance capacity and inhibition of in vitro lipoprotein oxidation in human serum samples. *J. Agric. Food Chem.* **2002**, *50*, 3050–3055. [[CrossRef](#)]
- Blasa, M.; Candiracci, M.; Accorsi, A.; Piacentini, M.P.; Albertini, M.C.; Piatti, E. Raw Millefiori honey is packed full of antioxidants. *Food Chem.* **2006**, *97*, 217–222. [[CrossRef](#)]
- Beretta, G.; Granata, P.; Ferrero, M.; Orioli, M.; Facino, R.M. Standardization of antioxidant properties of honey by a combination of spectrophotometric/fluorimetric assays and chemometrics. *Anal. Chim. Acta* **2005**, *533*, 185–191. [[CrossRef](#)]
- D’Arcy, R. *Antioxidants in Australian Floral Honeys: Identification of Health-Enhancing Nutrient Components: A Report for the Rural Industries Research and Development Corporation*; Bruce; Rural Industries Research and Development Corporation: Wagga Wagga, Australia, 2005; pp. 68–73.
- Inoue, K.; Murayama, S.; Seshimo, F.; Takeba, K.; Yoshimura, Y.; Nakazawa, H. Identification of phenolic compound in manuka honey as specific superoxide anion radical scavenger using electron spin resonance (ESR) and liquid chromatography with coulometric array detection. *J. Sci. Food Agric.* **2005**, *85*, 872–878. [[CrossRef](#)]
- Fahey, J.W.; Stephenson, K.K. Pinostrobin from honey and Thai ginger (*Boesenbergia pandurata*): A potent flavonoid inducer of mammalian phase 2 chemoprotective and antioxidant enzymes. *J. Agric. Food Chem.* **2002**, *50*, 7472–7476. [[CrossRef](#)]
- Frankel, S.; Robinson, G.E.; Berenbaum, M.R. Antioxidant capacity and correlated characteristics of 14 unifloral honeys. *J. Apic. Res.* **1998**, *37*, 27–31. [[CrossRef](#)]
- Schramm, D.D.; Karim, M.; Schrader, H.R.; Holt, R.R.; Cardetti, M.; Keen, C.L. Honey with high levels of antioxidants can provide protection to healthy human subjects. *J. Agric. Food Chem.* **2003**, *51*, 1732–1735. [[CrossRef](#)]
- Aljadi, A.M.; Kamaruddin, M.Y. Evaluation of the phenolic contents and antioxidant capacities of two Malaysian floral honeys. *Food Chem.* **2004**, *85*, 513–518. [[CrossRef](#)]
- Palma-Morales, M.; Huertas, J.R.; Rodríguez-Pérez, C. A Comprehensive Review of the Effect of Honey on Human Health. *Nutrients* **2023**, *15*, 3056. [[CrossRef](#)]
- Ranneh, Y.; Akim, A.M.; Hamid, H.A.; Khazaai, H.; Fadel, A.; Zakaria, Z.A.; Albuja, M.; Abu Bakar, M.F. Honey and its nutritional and anti-inflammatory value. *BMC Complement. Med. Ther.* **2021**, *21*, 30. [[CrossRef](#)]
- Leoni, V.; Panseri, S.; Giupponi, L.; Pavlovic, R.; Gianoncelli, C.; Sala, S.; Zeni, V.; Benelli, G.; Giorgi, A. Formal analyses are fundamental for the definition of honey, a product representing specific territories and their changes: The case of North Tyrrhenian dunes (Italy). *Sci. Rep.* **2023**, *13*, 17542. [[CrossRef](#)]
- Ahmed, A.; Tul-Noor, Z.; Lee, D.; Bajwah, S.; Ahmed, Z.; Zafar, S.; Syeda, M.; Jamil, F.; Qureshi, F.; Zia, F.; et al. Effect of honey on cardiometabolic risk factors: A systematic review and meta-analysis. *Nutr. Rev.* **2023**, *81*, 758–774. [[CrossRef](#)]
- Moniruzzaman, M.; Khalil, M.I.; Sulaiman, S.A.; Gan, S.H. Advances in the analytical methods for determining the antioxidant properties of honey: A review. *Afr. J. Tradit. Complement. Altern. Med. AJTCAM* **2012**, *9*, 36–42. [[CrossRef](#)]

15. Nurbianto, A.T.; Christian, T.F.; Surabaya, U.C. Marketing strategies through product awareness, service quality and product quality. *Devot. J. Community Serv.* **2024**, *5*, 461–470.
16. da Costa, I.F.; Toro, M.J.U. Evaluation of the antioxidant capacity of bioactive compounds and determination of proline in honeys from Pará. *J. Food Sci. Technol.* **2021**, *58*, 1900–1908. [[CrossRef](#)]
17. Codex Alimentarius. Revised Codex Standard for Honey, Standards and Standard Methods. *Codex Aliment. Comm. FAO/OMS* **2001**, *11*, 7.
18. Bogdanov, S.; Ruoff, K.; Oddo, L.P. Physico-chemical methods for the characterisation of unifloral honeys: A review. *Apidologie* **2004**, *38*, 67–76. [[CrossRef](#)]
19. Kirk, P.L. Kjeldahl Method for Total Nitrogen. *Anal. Chem.* **1950**, *22*, 354–358. [[CrossRef](#)]
20. Chakir, A.; Romane, A.; Marcazzan, G.L.; Ferrazzi, P. Physicochemical properties of some honeys produced from different plants in Morocco. *Arab. J. Chem.* **2016**, *9*, S946–S954. [[CrossRef](#)]
21. Singleton, V.L.; Orthofer, R.; Lamuela-Raventós, R.M. Analysis of total phenols and other oxidation substrates and antioxidants by means of folin-ciocalteu reagent. *Methods Enzymol.* **1999**, *299*, 152–178.
22. Ferreira, I.C.F.R.; Aires, E.; Barreira, J.C.M.; Estevinho, L.M. Antioxidant activity of Portuguese honey samples: Different contributions of the entire honey and phenolic extract. *Food Chem.* **2009**, *114*, 1438–1443. [[CrossRef](#)]
23. Hatano, T.; Kagawa, H.; Yasuhara, T.; Okuda, T. Two new flavonoids and other constituents in licorice root: Their relative astringency and radical scavenging effects. *Chem. Pharm. Bull.* **1988**, *36*, 2090–2097. [[CrossRef](#)]
24. Murphy, E.J.; Metcalfe, C.L.; Basran, J.; Moody, P.C.E.; Raven, E.L. Engineering the substrate specificity and reactivity of a heme protein: Creation of an ascorbate binding site in cytochrome c peroxidase. *Biochemistry* **2008**, *47*, 13933–13941. [[CrossRef](#)]
25. Frisch, M.J.; Trucks, G.W.; Schlegel, H.B.; Scuseria, G.E.; Robb, M.A.; Cheeseman, J.R.; Scalmani, G.; Barone, V.; Mennucci, B.; Petersson, G.A.; et al. *Gaussian 09, Revision B.01. Gaussian 09, Revis B01*; Gaussian, Inc.: Wallingford, CT, USA, 2009; pp. 1–20. Available online: <https://gaussian.com/g09citation/> (accessed on 10 April 2024).
26. Dennington, R.; Keith, T.; MillamSemichem, J.; Shawnee Mission, K. *GaussView, Version 5*; Semichem Inc.: Shawnee Mission, KS, USA, 2009.
27. Hameed, O.M.; Shaker, O.M.; Ben Slima, A.; Makni, M. Biochemical Profiling and Physicochemical and Biological Valorization of Iraqi Honey: A Comprehensive Analysis. *Molecules* **2024**, *29*, 671. [[CrossRef](#)]
28. Codex Alimentarius. STANDARD FOR HONEY CXS 12-19811 Adopted Adopted in 1981; Revised in 1987, 2001; Amended in 2019, 2022. *Int. Foods Standars.* **2022**.
29. Kahraman, K.; Göcenler, O.; Dağ, Ç. Characterization of Turkish Pine honey and differentiation from floral honeys by NMR spectroscopy and chemometric analysis. *J. Food Compos. Anal.* **2024**, *127*, 105983. [[CrossRef](#)]
30. Mehdi, R.; Zrira, S.; Vadalà, R.; Nava, V.; Condurso, C.; Cicero, N.; Costa, R. A Preliminary Investigation of Special Types of Honey Marketed in Morocco. *J. Exp. Theor. Anal.* **2023**, *1*, 1–20. [[CrossRef](#)]
31. Prica, N.; Baloš, M.Ž.; Jakšić, S.; Mihaljev, Ž.; Kartalović, B.; Babić, J.; Savić, S. Moisture and Acidity as Indicators of the Quality of Honey Originating from Vojvodina Region. *Arch. Vet. Med.* **2015**, *7*, 99–109. [[CrossRef](#)]
32. Azeredo, L.D.C.; Azeredo, M.A.A.; De Souza, S.R.; Dutra, V.M.L. Protein contents and physicochemical properties in honey samples of *Apis mellifera* of different floral origins. *Food Chem.* **2003**, *80*, 249–254. [[CrossRef](#)]
33. Pauliuc, D.; Oroian, M.; Ciursă, P. Organic acids content, sugars content and physicochemical parameters of Romanian acacia honey. *Ukr. Food J.* **2021**, *10*, 158–170. [[CrossRef](#)]
34. Pasiás, I.N.; Kiriakou, I.K.; Proestos, C. HMF and diastase activity in honeys: A fully validated approach and a chemometric analysis for identification of honey freshness and adulteration. *Food Chem.* **2017**, *229*, 425–431. [[CrossRef](#)]
35. Bodó, A.; Radványi, L.; Kőszegi, T.; Csepregi, R.; Nagy, D.U.; Farkas, Á.; Kocsis, M. Quality Evaluation of Light- and Dark-Colored Hungarian Honeys, Focusing on Botanical Origin, Antioxidant Capacity and Mineral Content. *Molecules* **2021**, *26*, 2825. [[CrossRef](#)]
36. Khalil, M.I.; Moniruzzaman, M.; Boukraâ, L.; Benhanifia, M.; Islam, M.A.; Islam, M.N.; Sulaiman, S.A.; SiewHua, G. Physicochemical and antioxidant properties of algerian honey. *Molecules* **2012**, *17*, 11199–11215. [[CrossRef](#)]
37. Pauliuc, D.; Dranca, F.; Oroian, M. Antioxidant activity, total phenolic content, individual phenolics and physicochemical parameters suitability for Romanian honey authentication. *Foods* **2020**, *9*, 306. [[CrossRef](#)]
38. Jasicka-Misiak, I.; Poliwoda, A.; Dereń, M.; Kafarski, P. Phenolic compounds and abscisic acid as potential markers for the floral origin of two Polish unifloral honeys. *Food Chem.* **2012**, *131*, 1149–1156. [[CrossRef](#)]
39. Özkök, A.; D’arcy, B.; Sorkun, K. Total Phenolic Acid and Total Flavonoid Content of Turkish Pine Honeydew Honey. *J. ApiProduct. ApiMedical. Sci.* **2010**, *2*, 65–71. [[CrossRef](#)]
40. Miranda, I.R.; Acevedo-Fernández, J.; Negrete-Leon, E.; Betancur-Ancona, D.A.; Moguel-Ordoñez, Y.B. In Vivo Wound-Healing and Anti-Inflammatory Activities of Honey Produced by *Melipona beecheii* Bees. *Jundishapur J. Nat. Pharm. Prod.* **2024**, *19*, e143682.
41. Khalil, M.I.; Alam, N.; Moniruzzaman, M.; Sulaiman, S.A.; Gan, S.H. Phenolic acid composition and antioxidant properties of Malaysian honeys. *J. Food Sci.* **2011**, *76*, C921–C928. [[CrossRef](#)]
42. Sweilam, S.H.; Abdel Bar, F.M.; Foudah, A.I.; Alqarni, M.H.; Elattal, N.A.; El-Gindi, O.D.; El-Sherei, M.M.; Abdel-Sattar, E. Phytochemical, Antimicrobial, Antioxidant, and In Vitro Cytotoxicity Evaluation of *Echinops erinaceus* Kit Tan. *Separations* **2022**, *9*, 447. [[CrossRef](#)]

43. Taibi, M.; Elbouzidi, A.; Ou-Yahia, D.; Dalli, M.; Bellaouchi, R.; Tikent, A.; Roubi, M.; Gseyra, N.; Asehrou, A.; Hano, C.; et al. Assessment of the Antioxidant and Antimicrobial Potential of *Ptychotis verticillata* Duby Essential Oil from Eastern Morocco: An In Vitro and In Silico Analysis. *Antibiotics* **2023**, *12*, 655. [[CrossRef](#)]
44. Ludington, J.L. Protein binding site analysis for drug discovery using a computational fragment-based method. *Methods Mol. Biol.* **2015**, *1289*, 145–154.
45. Ismail, C.M.K.H.; Abdul Hamid, A.A.; Abdul Rashid, N.N.; Lestari, W.; Mokhtar, K.I.; Mustafa Alahmad, B.E.; Razake, M.R.M.A.; Ismail, A. An ensemble docking-based virtual screening and molecular dynamics simulation of phytochemical compounds from Malaysian Kelulut Honey (KH) against SARS-CoV-2 target enzyme, human angiotensin-converting enzyme 2 (ACE-2). *J. Biomol. Struct. Dyn.* **2024**, 1–30. [[CrossRef](#)]
46. Sun, Z.; Lin, Y.; Yang, H.; Zhao, R.; Zhu, J.; Wang, F. Characterization of honey-like characteristic aroma compounds in Zunyi black tea and their molecular mechanisms of interaction with olfactory receptors using molecular docking. *LWT* **2024**, *191*, 115640. [[CrossRef](#)]
47. Bazaid, A.S.; Alsolami, A.; Patel, M.; Khateb, A.M.; Aldarhami, A.; Snoussi, M.; Almusheet, S.M.; Qanash, H. Antibiofilm, Antimicrobial, Anti-Quorum Sensing, and Antioxidant Activities of Saudi Sidr Honey: In Vitro and Molecular Docking Studies. *Pharmaceutics* **2023**, *15*, 2177. [[CrossRef](#)]
48. Abu-Rayyan, A.; Suleiman, M.; Daraghme, A.; Al Ali, A.; Zarruk, A.; Kumara, K.; Sawafta, A.; Warad, I. Synthesis, characterization, E/Z-isomerization, DFT, optical and 1BNA docking of new Schiff base derived from naphthalene-2-sulfonylhydrazide. *Moroccan J. Chem.* **2023**, *11*, 613–622.
49. Toubi, Y.; Abridgach, F.; Radi, S.; Souana, F.; Hakkou, A.; Alsayari, A.; Bin Muhsinah, A.; Mabkhot, Y.N. Synthesis, Antimicrobial Screening, Homology Modeling, and Molecular Docking Studies of a New Series of Schiff Base Derivatives as Prospective Fungal Inhibitor Candidates. *Molecules* **2019**, *24*, 3250. [[CrossRef](#)]
50. Kumar, S.; Saini, V.; Maurya, I.K.; Sindhu, J.; Kumari, M.; Kataria, R.; Kumar, V. Design, synthesis, DFT, docking studies and ADME prediction of some new coumarinyl linked pyrazolylthiazoles: Potential standalone or adjuvant antimicrobial agents. *PLoS ONE* **2018**, *13*, e0196016. [[CrossRef](#)]
51. Youssefi, Y.; Oucheikh, L.; Ou-Ani, O.; Jabha, M.; Oubair, A.; Znini, M.; Ebenso, E.E.; Hammouti, B. Synthesis, Characterization and Corrosion Inhibition Potential of Olefin Derivatives for Carbon Steel in 1M HCl: Electrochemical and DFT Investigations. *Moroccan J. Chem.* **2023**, *11*, 155–187.
52. El Hadki, A.; El Hadki, H.; Tazi, R.; Komiha, N.; Zrineh, A.; El Hajjaji, S.; Kabbaj, O.K. DFT and Molecular docking study of natural molecules proposed for COVID-19 treatment. *Moroccan J. Chem.* **2021**, *9*, 198–209.
53. El-Shamy, N.T.; Alkaoud, A.M.; Hussein, R.K.; Ibrahim, M.A.; Alhamzani, A.G.; Abou-Krishna, M.M. DFT, ADMET and Molecular Docking Investigations for the Antimicrobial Activity of 6,6'-Diamino-1,1',3,3'-tetramethyl-5,5'-(4-chlorobenzylidene) bis[pyrimidine-2,4(1H,3H)-dione]. *Molecules* **2022**, *27*, 620. [[CrossRef](#)]
54. Edim, M.M.; Enudi, O.C.; Asuquo, B.B.; Louis, H.; Bisong, E.A.; Agwupuye, J.A.; Chioma, A.G.; Odey, J.O.; Joseph, I.; Bassey, F.I. Aromaticity indices, electronic structural properties, and fuzzy atomic space investigations of naphthalene and its aza-derivatives. *Heliyon* **2021**, *7*, e06138. [[CrossRef](#)] [[PubMed](#)]
55. Moran, G.S.; Cardona, W.V.; Candia, L.G.; Mendoza-Huizar, L.H.; Abdizadeh, T. Identification of Novel Coumarin Based Compounds as Potential Inhibitors of the 3-Chymotrypsin-Like Main Protease of SARS-CoV-2 Using Dft, Molecular Docking and Molecular Dynamics Simulation Studies. *J. Chil. Chem. Soc.* **2022**, *67*, 5521–5536. [[CrossRef](#)]
56. Okulik, N.; Jubert a, H. Theoretical Analysis of the Reactive Sites of Non-steroidal Anti-inflammatory Drugs. *Internet Electron. J. Mol. Des.* **2005**, *4*, 17–30.
57. Panicker, C.Y.; Varghese, H.T.; Narayana, B.; Divya, K.; Sarojini, B.K.; War, J.A.; Van Alsenoy, C.; Fun, H.K. FT-IR, NBO, HOMO-LUMO, MEP analysis and molecular docking study of Methyl N-([2-(2-methoxyacetamido)-4-(phenylsulfanyl)phenyl] amino) [(methoxycarbonyl) imino] methyl) carbamate. *Spectrochim. Acta A Mol. Biomol. Spectrosc.* **2015**, *148*, 29–42. [[CrossRef](#)]

Disclaimer/Publisher's Note: The statements, opinions and data contained in all publications are solely those of the individual author(s) and contributor(s) and not of MDPI and/or the editor(s). MDPI and/or the editor(s) disclaim responsibility for any injury to people or property resulting from any ideas, methods, instructions or products referred to in the content.